Reliable Communications in Aerial Sensor Networks by Using A Hybrid Antenna

Kai Li Nadeem Ahmed Salil S. Kanhere Sanjay Jha

University of New South Wales, Australia
{kail, nahmed, salilk, sanjay}@cse.unsw.edu.au

Technical Report
UNSW-CSE-TR-201211
May 2012

THE UNIVERSITY OF
NEW SOUTH WALES

School of Computer Science and Engineering
The University of New South Wales
Sydney 2052, Australia

Abstract

An AWSN composed of bird-sized Unmanned Aerial Vehicles (UAVs) equipped with sensors and wireless radio, enables low cost high granularity three-dimensional sensing of the physical world. The sensed data is relayed in real-time over a multi-hop wireless communication network to ground stations. The following characteristics of an AWSN make effective multi-hop communication challenging - (i) frequent link disconnections due to the inherent dynamism (ii) significant inter-node interference (iii) three dimensional motion of the UAVs. In this paper, we investigate the use of a hybrid antenna to accomplish efficient neighbor discovery and reliable communication in AWSNs. We propose the design of a hybrid Omni Bidirectional ESPAR (O-BESPAR) antenna, which combines the complimentary features of an isotropic omni radio (360 degree coverage) and directional ESPAR antennas (beamforming and reduced interference). Control and data messages are transmitted separately over the omni and directional modules of the antenna, respectively. Moreover, a communication protocol is presented to perform fast neighbor discovery and beam steering. We present results from extensive simulations then consider three different real-world AWSN application scenarios and empirical aerial link characterization and show that the proposed antenna design and protocol reduces the packet loss rate and end to end delay by up to 54% and 49 seconds respectively, and increases the goodput by up to 33%, as compared to a single omni or ESPAR antenna.

1 Introduction

In recent years, mobile sensors have been successfully adopted for terrestrial [10] and ocean monitoring [26]. The next logical step in their evolution is to enable mobile sensors to explore the aerial dimension, i.e., engineering Unmanned Aerial Vehicles (UAVs) with sensors and wireless radios to form an Aerial Wireless Sensor Network (AWSN). The idea of equipping a UAV with sensors is not new. In fact, most UAVs have in-built sensors such as accelerometers and gyroscopes, which measure various parameters related to the vehicle‘s motion to assist with autonomous flying. UAVs have been fitted with additional sensors such as cameras for collecting data about the physical environment. The sensed data is relayed to a ground station by equipping the MAV with a 802.11 or Zigbee radio. Even though this enables real-time collection of data, the area that can be monitored is limited to the range of the wireless radio. However, if the MAVs can communicate with each other wirelessly and create a multi-hop aerial network, then the sensed information can be relayed back to a distant base station in real-time. Such an aerial network would significantly extend the coverage range, thus enabling access to remote areas. It is thus no surprise that AWSNs are being increasingly used in a variety of applications such as precision agriculture [25], environmental monitoring [23] and search and rescue operations in dangerous areas [12].

On surface, this kind of network may appear to be very similar to ad-hoc networks, extensively studied by the networking community. However, one of the major distinction of AWSNs is the dynamism and timescale where the vehicles may connect/disconnect with each other for a very short duration of time. Given the short connection opportunities, it is critical that a UAV can quickly detect the presence of another UAV in its communication range (i.e. neighbor discovery) so as to maximise the duration for which data can be transferred [7]. Moreover, in a typical AWSN [9], the node density can be fairly high, leading to excessive interference, thus affecting the network throughput. The inter-node interference can also impact the neighbour discovery mechanism (e.g., data packets may collide with control packets intended for neighbour discovery), which in turn can further reduce the overall network throughput. Another unique property of AWSNs is that that the nodes can move in all three dimensions. It has been shown that the difference in the altitude of the UAVs can have a significant effect on the signal strength variability between transmitter-receiver pairs for omni-directional radios, due to the relative monopole antenna orientation [18].

In this paper, we explore the idea of using directional antennas to overcome the aforementioned challenges. By radiating greater power in one or more directions, such antennas are known to reduce interference from unwanted sources and subsequently increase throughput. In particular, we seek to build upon the popular Electronically Steerable Passive Array Radiator (ESPAR) antenna [16] for a number of reasons. First, it can achieve directional transmission by beamforming so that the signal is transmitted exactly within the beam width, thus limiting interference. The antenna has a single active element at the center and is surrounded by six reactively loaded parasitic elements. Through changing the reactances of the elements, a signal beam which points to the specified direction and relevant nulls can be formed. This creates a larger radiation intensity in the desired direction, thus extending the range over which the signal is transmitted. Second, the small form factor (120mm diameter and 61.5mm height for a seven-element ESPAR) [22] and low-power operation, make it well-suited for mounting on a UAV. Third, is its ability to create desired transmit radiation patterns in real-time [5], which is particularly important for the dynamism inherent in an AWSN. Finally, it has also been shown that ESPAR can generate 360 degree continuous beam and null steering [21], which makes it suitable for the 3D flight of the UAVs.

However, incorporating the ESPAR antenna in an AWSN presents several non-trivial challenges. Although an ESPAR antenna is capable of generating multiple lobes in different directions, the gain in each direction reduces a compared with a single directional ESPAR [11]. Also such an antenna causes unnecessary interference as it transmits in multiple directions. Therefore, for this work, we consider a single directional ESPAR antenna. Neighbor discovery with a single beam directional ESPAR can incur significant delays. This is because, scanning the entire neighbourhood of a node can only be achieved by sweeping the directional beam in 360 degrees. Note that, the beams of both neighboring UAVs need to be aligned with each other for neighbor discovery to be successful. Despite, the quick operation of the ESPAR antenna, this process can use up precious seconds (excluding the delay incurred for exchanging handshaking messages, once the beams are aligned), which could otherwise be used for data transfer. In the worst case, a data exchange opportunity may be completely lost if the two beams are unable to encounter each other during the scanning process. Moreover, the presence of a single directional antenna only permits a UAV to communicate with a single neighbour at any given time.

To address these issues, in this paper, we leverage the complimentary properties of omni-directional (360 degree coverage) and directional antennas (discussed earlier) and propose the design of a hybrid antenna. In particular, we propose to use the isotropic omni antenna as a control channel to quickly achieve neighbor discovery, and two directional antennas as the data channel to achieve greater throughput and reduced interference. As such, we refer to our proposed hybrid design as Omni Bi-directional ESPAR (O-BESPAR) antenna. The two independent directional beams permit a node to transmit and receive simultaneously, hence the name bi-directional. We also propose a communication protocol that incorporates an efficient neighbor discovery mechanism which not only allows UAVs to discover each other rapidly but also enables quick alignment of directional beams to maximise the data transfer opportunities. According to our communication protocol, sender UAV broadcasts control messages through the omni module in order to exchange location information with receiver. After both beams are steered to each other, the data transmission commences over the directional module. However, the transmission range of the omni antenna is much smaller than the directional ESPAR module. As such, if no neighbor is found by the broadcast of the omni module, the communication protocol will use the directional module to perform bi-directional beam sweeping. Each beam covers 180 degrees so that the scanning delay is minimized.

In summary, the following are our specific contributions:

- To the best of our knowledge, this is the first paper to propose an omni and bi-directional hybrid antenna structure.
- We propose a communication protocol that achieves efficient neighbour discovery for the proposed hybrid antenna. We exclusively use the omni antenna as a control plane for neighbor discovery. The two directional

beams are only invoked as a backup mechanism during neighbour discovery to address the disparity in the communication range of the omni and directional antennas. These beams are primarily used as the data plane for reducing interference and achieving increased throughput.

- We conduct extensive simulations to analyze the performance of the proposed O-BESPAR antenna and communication protocol. In our experiments we consider three different scenarios which reflect real-world use cases for AWSNs and also incorporate realistic 3D link characterizations based on our prior field experiments with UAVs [3]. Our results show that our hybrid antenna can on average *halve* the packet loss and increase the goodput by 33% as compared to using omni-directional antennas. Moreover, in comparison with a single ESPAR antenna, the hybrid design increases the goodput by 18% and decreases the end to end delay by 49%.

The rest of the paper is organized as follows. Section II reviews the related work. Section III describes the proposed hybrid O-BESPAR antenna model and the associated communication protocol. In Section IV, we present simulation results from three typical real-world AWSN scenarios to demonstrate the efficacy of the proposed ideas. Finally, the paper is concluded in Section V.

2 Related Work

In this section, we review related research on the use of directional antennas for neighbor discovery and reducing interference in wireless ad-hoc and mobile networks.

Research in [8] has clearly demonstrated the efficacy of using directional antennas in wireless ad hoc networks. Their results show that the longer transmission distance of directional antennas can increase the network throughput capacity and also reduce the transmission delay. In addition, recent work [17] has found that directional antennas achieve better energy efficiency than traditional omnidirectional antenna as the former improves signal to noise ratio by power centralization. The above results lend promise to the idea of using directional antennas in AWSNs, provided the practicalities (form-factor and power consumption) can be addressed.

Directional antenna and beam steering are used to improve connectivity duration and network throughput for moving vehicles [20]. In their work, a framework called *MobiSteer* is proposed, which selects the best roadside access point and beam combination based on physical layer data rate. The beam of the directional antenna on mobile nodes is steered to different access points as the vehicle travels along its route. However, *MobiSteer* can only work for infrastructure based networks. Their framework cannot be applied to AWSNs.

A directional antenna model with MAC protocol are proposed to reduce inter-node interference in mobile ad hoc networks [19]. In their model, each mobile node is equipped with a number of directional antennas to cover 360 degrees. However, the non-overlapping beams generated by the directional antennas have fixed directions. The MAC protocol has to broadcast RTS in all directions to find a neighbor. The node will not select which directional antenna to communicate with until it receives a CTS response. Besides, it is assumed that all nodes are able to maintain their orientation at all times, irrespective of their motion. This assumption is not valid in an AWSN since UAVs move in all three dimensions. Moreover, it is not practical to mount a large number of directional antennas on a UAV both from the point of view of power consumption and form factor.

In [4], an adaptive MAC protocol using ESPAR antenna is proposed to maintain a neighborhood angle-SINR table so that each node can know how to set transmission direction. Furthermore, a modified link-state based routing protocol captures the network status periodically for directional routing. As such, each node should be aware of the entire network topology. This requirement would be difficult to meet in an AWSN since the network topology is highly dynamic and inter-node contact durations are very short. As such, setting up such a table would be quite challenging.

3 O-BESPAR Antenna Design and Communication Protocol

In this section, we first present the antenna design of the proposed O-BESPAR antenna. Next, we present the communication protocol for optimizing the usage of the hybrid antenna.

3.1 Antenna Structure

In order to generate two independent and separate main lobes, a twelve-element bi-directional ESPAR antenna structure is proposed. Specifically, this is a structural improvement of the seven-element ESPAR antenna, the optimizations for which are covered in [22]. The 360 degrees radiation pattern experiments for this antenna have been reported in [16]. The proposed O-BESPAR antenna design is based on this twelve-element bi-directional ESPAR antenna structure. It is able to broadcast neighbor discovery messages using the omni antenna. Once the receiver UAV is found, transmitter will simply change the DC voltage across varactors of the passive antenna elements to control the radiation pattern of the directional module [13]. Following this, one of the O-BESPAR main lobes can be directed to the receiver for data transmission.

The structure and 3D coverage pattern of the directional module of O-BESPAR are shown in Figure 3.1 and 2. The active and passive elements are marked in red and black, respectively. The parameters R_p, R_g, h_t and h_g represent passive elements radius, ground skirt radius, all the elements height and ground skirt height, respectively. Both of the active elements work at 2.4GHz and both of them are encircled by six passive elements.

Figure 2 shows the radiated beam pattern for an ESPAR antenna. ϕ_1, ϕ_2 and θ_1, θ_2 stand for angle of the beam in horizontal plane and vertical plane. ϕ_1 covers from 0 to π and the value of ϕ_2 is in $[\pi, 2\pi]$. In vertical plane the angle of coverage θ_1 and θ_2 are equal to antenna beam width. The default values θ_1 and θ_2 of directional module are 0 and π.

It is well known that the antenna gain G is defined as,

$$G = e \cdot D \tag{3.1}$$

where e is the antenna efficiency and D is its directivity [6]. The ESPAR antenna

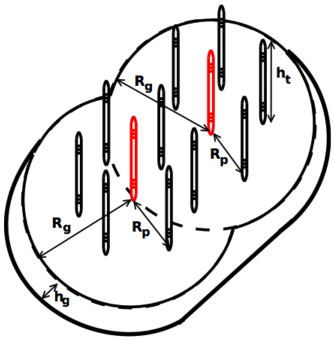

Figure 3.1: Directional module of O-BESPAR antenna structure

gain is calculated by,

$$G = (1 - |S_{11}|^2) \cdot D \tag{3.2}$$

$$S_{11} = \frac{Z_{in} - Z_s}{Z_{in} + Z_s} \tag{3.3}$$

where S_{11} is antenna reflection coefficient, Z_{in} is antenna input impedance and Z_s is characteristic impedance of the transmission line. Since the directional module of O-BESPAR has two independent main lobes, the gain in each direction of the main lobe would be identical.

According to the experimental results in [14], a single ESPAR antenna has 360 degree beam and null steering in the azimuth with a maximum achievable directivity of $8.73dB_i$. It is denoted that the antenna gain difference between main lobe of single ESPAR antenna and omni antenna is $G_{ESPAR} \approx 8 \cdot G_{Omni}$ assuming we have $G_{Omni} = 1dB_i$.

If λ represents the wavelength, based on the optimization of ESPAR [22] for 2.4GHz, we have $R_p = 0.308\lambda = 38.5, R_g = 0.480\lambda = 60mm, h_t = 0.216\lambda = 27mm, h_g = 0.276\lambda = 34.5mm$. Explicitly, the length of O-BESPAR antenna is $3R_g = 180mm$, the width equals $2R_g = 120mm$ and the height is $h_t + h_g = 61.5mm$. These dimensions are thus suitable for mounting the O-BESPAR antenna on a bird sized UAV. The power consumption of an ESPAR antenna is very low as compared with a physically steerable directional antenna. This again is an added advantage as power consumption is of paramount importance for extending the flight time of the battery operated UAV.

3.2 Communication Protocol

Before we describe the protocol, we first list some of the assumptions we make. We assume that each UAV is equipped with a GPS receiver and an altitude sensor such as a barometer (we have found that GPS cannot accurately indicate the altitude). Moreover, we assume that the GPS and altitude readings are accurate. We also neglect the delay incurred in steering and aligning the directional beams but account for the delay in beam sweeping employed in the backup neighbor discovery mechanism. We also assume that each UAV knows the location of the base station on initialization. While, we acknowledge that some of these assumptions may not hold in the real-world, these simplifications are necessary for a tractable design. In our future work, we plan to design real

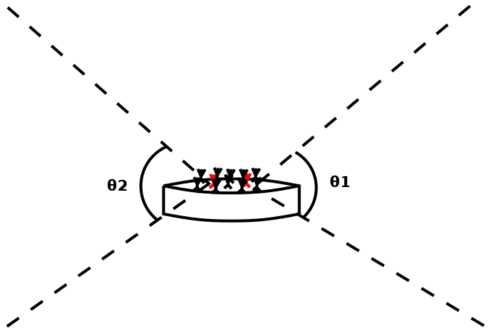

(a) Directional module of O-BESPAR antenna coverage

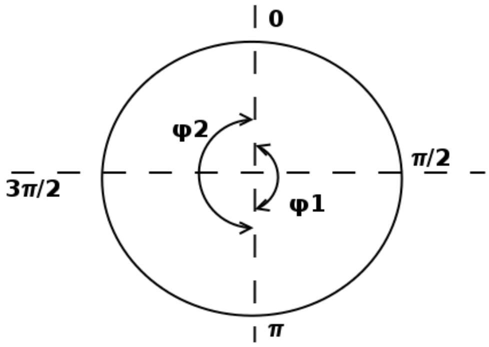

(b) Horizontal plane of O-BESPAR directional module

Figure 3.2: Coverage of O-BESPAR antenna directional module in 3D

hardware based on the proposed design and conduct field experiments. This will allow us to investigate the impact of relaxing these assumptions on the performance of our antenna.

We have designed this communication protocol with two main objectives. Firstly, to perform efficient neighbor discovery in AWSN equipped with O-BESPAR antennas. Secondly, to reduce interference during data transmission phase utilizing the bi-directional beams for the antenna. Our communication protocol employs handshaking mechanism through the use of *HELLO* and *ACK* messages. *HELLO* messages contains the sender UAV ID, its current 3D location (x,y,z) coordinates and the antenna module in use. These neighbor discovery messages are first sent out through the omni module of the antenna. Given that the omni antenna has a limited range, these message may or may not reach a neighbor UAV. If a UAV receives a *HELLO* message, it would check which antenna module has been used by the sender UAV. In case the message was sent though the omni antenna, it would generate an *ACK* message back to the sender UAV employing the omni antenna. Now both Sender and Receiver UAV can calculate the direction of their main lobes such that they can locate their communicating neighbor by directing their directional antenna main lobes. The

UAVs calculate the angle $(\phi, \theta)_{UAV}$ between the neighbor and itself as follows,

$$(\phi, \theta)_{UAV} = \arctan\left(\frac{z_2 - z_1}{\sqrt{(x_2 - x_1)^2 + (y_2 - y_1)^2}}\right) \tag{3.4}$$

In case, there is no response to the *HELLO* messages sent out through the omni module, the Sender UAV employs the fall-back mechanism and activates the neighbor discovery through the directional beam sweeping. For the UAV that is one-hop away from the base station. since the location of the base station is already known, the UAV would only employ beam sweeping through one of the directional beam, towards the direction of the base station. The resulting *HELLO* message marks antenna module as directional. The Receiver UAV on reception of this *HELLO* Message, first steers its main lobe towards the Sender UAV and then sends out the *ACK* message. Both Sender and Receiver are thus able to locate each other if they are reachable either through the omni antenna or directional beam. Once the handshaking is completed, the data transmission phase can begin. This procedure is repeated hop by hop. UAVs employ different main lobes for sending and receiving data simultaneously for different hops. The pseudo-code for the proposed protocol is shown in Algorithm 1.

4 Simulations and Results

We implemented the O-BESPAR antenna and the communication protocol in simulations to evaluate its performance compared to single omni-directional antenna. We use the NS-2 simulator. The performance evaluation is based on three criteria: per hop packet loss rate, end to end delay and the goodput, which reflects the total data transmitted by each UAV to the base station.

4.1 Scenarios

We employ three different AWSN network topologies which reflect real-world AWSN applications. Figure 4.1 illustrates an example of an ant-based network which is used to create and maintain aerial ad-hoc network between rescuers to share survivor's information [15]. In Figure 4.1, a target area of size 150m X 100m is sub-divided into three sub-areas each of size 50m X 100m. Three UAVs fly in the target area one in each sub-area following random walk to collect data. The blue nodes are UAVs, the big circles represents the omni module transmission ranges and the dash lines with arrows shows the UAV moving path. The UAVs fly at a fixed altitudes. The height of UAV-1, UAV-2 and UAV-3 are defined to be $H_{UAV1} = 5m, H_{UAV2} = 10m, H_{UAV3} = 15m$. The base station is placed at location (0,50) at a height of 1.5 meters above the ground. Only UAV-1 can communicate with the base station directly. Data from UAV-3 and UAV-2 is relayed back to the base station through multi-hop. All UAVs fly at the same speed. In our simulations, we vary the speed of the UAVs from 0.6 m/s to 2.4 m/s (in steps of 0.2 m/s). At higher speeds, the UAVs disconnect/connect with each other more frequently. This allows us to study the impact of increasing dynamism on the packet loss rate, goodput and end to end delay.

Figure 4.2 shows the second network topology, which is often used in co-operative UAV search and rescue operations [24] and surveillance patrol. The

Algorithm 1 O-BESPAR Communication Protocol

Notations:
U_i: current UAV
U_j: neighbor UAV
$(\phi, \theta)_{UAV}$: the angle between transmitter and receiver UAV
Procedure:

if U_i has data to transmit **then**
  Broadcast *HELLO* through omni module
  if U_j received *HELLO* through omni module **then**
    Extract UAVId and calculate $(\phi, \theta)_{UAV}$
    Reply *ACK* through omni module and direct one beam to the U_i
    if *ACK* is received by omni module of U_i **then**
      Calculate $(\phi, \theta)_{UAV}$ and direct one beam to the U_j
      Start transmitting data through directional module
    end if
  else
    U_i sends out *HELLO* through directional module
    if U_j received *HELLO* through directional module **then**
      Extract UAVId and calculate $(\phi, \theta)_{UAV}$
      Reply *ACK* message through directional module and direct one beam to the U_i
    end if
    if *ACK* is received by U_i **then**
      Start transmitting data through directional module
    else
      Sweep the beam to another direction
    end if
    if No *ACK* is received by both antenna modules **then**
      U_i stores the data into a buffer
    end if
  end if
end if

target area in this case is divided into cells with UAVs moving up and down along fixed paths. In this scenario, the size of area is 90m X 200m. The rest of the parameters are similar to those in Scenario 1.

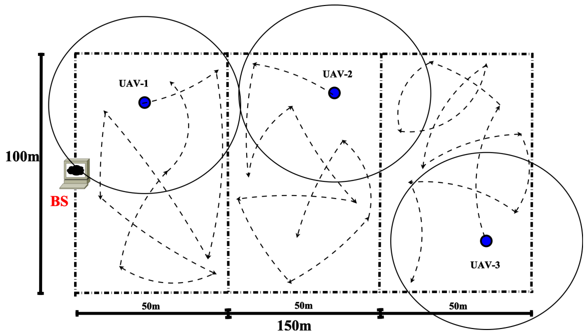

Figure 4.1: Random walk in grid topology

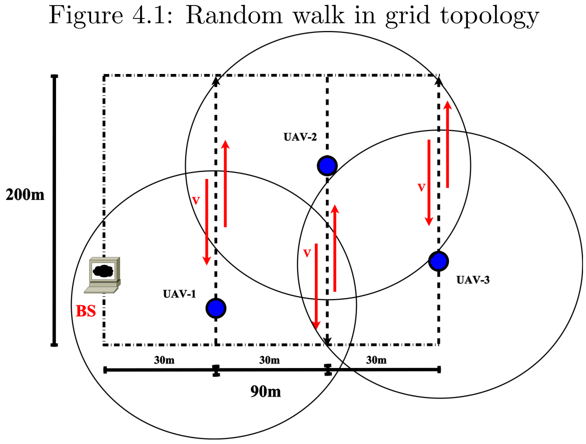

Figure 4.2: UP-DOWN movement

The third network topology is inspired by a UAV formation flight research discussed in [27], where a mobility model and a series of simulations are proposed to find out the network constrains. Figure 4.3 shows three UAVs flying in a 200m X 200m area following random walk model. The location of the base station and the heights of the UAVs are similar to those in the first two scenarios. Unlike, the two previous scenarios, we assume that each UAV chooses a random speed between 0.6m/s and 2.4m/s, so as to be consistent with the application in [27].

4.2 Network Configurations

Our purpose is to simulate and compare three antenna models, omni antenna, normal ESPAR antenna and O-BESPAR antenna. Based on the typical flight time of off-the-shelf UAV products [2], the simulation period is set as 15 minutes. Both the UAVs and the base station work in 2.4GHz frequency band. UAV data sampling rate is fixed at 5 samples/s implying that five *HELLO* messages are sent per sec to search for the neighbor UAVs.

We utilize Two-ray ground path loss model as the propagation model in the simulation. If the transmission power P_t, antenna gain of transmitter G_t,

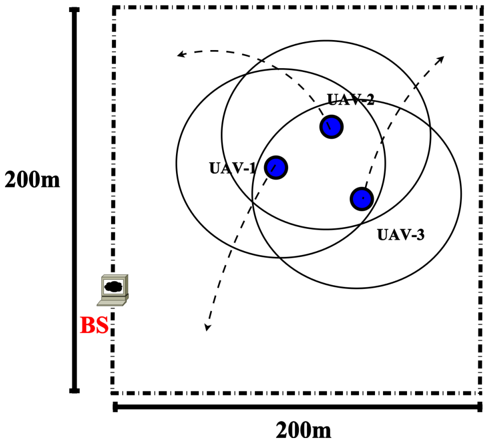

Figure 4.3: Random walk in square topology

antenna gain of receiver G_r, distance d, antenna heights H_t and H_r are all known, the receiving power P_r can be calculated by

$$P_r = \frac{P_t G_t G_r H_t^2 H_r^2}{d^4} \tag{4.1}$$

In our prior work [3], we have demonstrated using empirical measurements that the sensor node's antenna is not completely omni-directional in a 3D scenario. The antenna orientation and multi-path fading due to ground reflections have a significant influence on the link quality in an AWSN. The length of the line of sight path (L_{los}) and the length of the ground reflected wave (L_{grw}) between the sender and receiver are given by,

$$L_{los} = \sqrt{d^2 + (H_t - H_r)^2} \tag{4.2}$$

$$L_{grw} = \sqrt{d^2 + (H_t + H_r)^2} \tag{4.3}$$

So the phase difference or shift between the two waves is given by

$$\varphi = \frac{(L_{grw} - L_{los})2\pi}{\lambda} \tag{4.4}$$

Thus, the multi-path fading causes constructive or destructive interference to the original signal because of φ. Based on the link characterization experimental results reported in [3], for our simulations, we altered the P_r given by Two Ray Ground to include the effect of antenna orientation as well as empirically observed propagation loss.

We assume that the antenna height H_t, H_r and transmission power P_t are the same for omni and directional and that the same type of antenna is used for the sender and receiver. The transmission distance d would thus be different to achieve the same receiving power P_r. For omni module,

$$d_{Omni} = \sqrt[4]{\frac{P_t G_{t\_Omni} G_{r\_Omni} H_t^2 H_r^2}{P_r}} \tag{4.5}$$

For directional module,

$$d_{ESPAR} = \sqrt[4]{\frac{P_t G_{t\_ESPAR} G_{r\_ESPAR} H_t^2 H_r^2}{P_r}} \tag{4.6}$$

The relative transmission distance is then given by

$$\frac{d_{Omni}}{d_{ESPAR}} = \sqrt[4]{\frac{G_{t\_Omni} G_{r\_Omni}}{G_{t\_ESPAR} G_{r\_ESPAR}}} \tag{4.7}$$

$$\frac{d_{Omni}}{d_{ESPAR}} = \sqrt[2]{\frac{G_{Omni}}{G_{ESPAR}}} \tag{4.8}$$

Since $G_{ESPAR} \approx 8 \cdot G_{Omni}$ (see Section III), the transmission distance relationship is

$$d_{ESPAR} = \sqrt{8} \cdot d_{Omni} \tag{4.9}$$

We define the omni transmission range as 35m. The transmission range for the main lobe of the directional beam calculated according to Equation 13, is 98m.

4.3 Simulation Results

In the first random walk scenario, the packet loss rate, goodput and end to end delay of the 3 antenna models under consideration are simulated for different flying speeds (0.6m/s to 2.4m/s in steps on 0.2m/s). Each simulation is repeated for 20 times. In Figure 4.4 we present average results with 95% confidence intervals.

Figure 4.4(a), (b) and (c) show that the packet loss rate (with 95% confidence interval) of two UAV links and the UAV-base station link with omni antenna increases with increase in flying speed. About 58% of data from UAV-3 to UAV-2, 42% from UAV-2 to UAV-1 and 30% from UAV-1 to base station are lost at the speed of 2.4m/s. At the low speed of 0.6m/s, packet loss is about 5% to 22%. At high speeds, UAVs fly across the transmission ranges of each other frequently, so the contact time is less. As the sender transmits all of the buffered data when it receives the ACK, the transmitted data will be lost if one of them flies out of the range.

For O-BESPAR antenna, the packet loss rate is much less than the omni's due to the directional transmission. Even at the high speed of 2.4m/s, less than 5% packets are lost. At high speed, the packet loss rate of single ESPAR is about 3% higher than O-BESPAR antenna.

Figure 4.4(d), (e) and (f) illustrate the data packets which are actually transmitted by UAVs (goodput). The sender UAV has to store data into its buffer if it does not find the receiver. O-BESPAR antenna transmits more data packets compared to omni antenna due to its longer transmission distance. It also transmits 18% more data packets than single ESPAR antenna due to its faster neighbor discovery mechanism because of the omni module.

Figure 4.5 presents the end to end delay of packet transmission. O-BESPAR antenna achieves much smaller end to end delay which is about 32 seconds than ESPAR and omni antenna benefiting from the large transmission range and the beam forming in two directions.

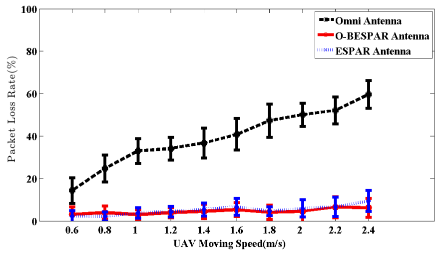

(a) Packet loss rate of link UAV-3 to UAV-2

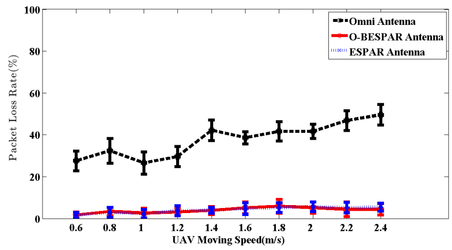

(b) Packet loss rate of link UAV-2 to UAV-1

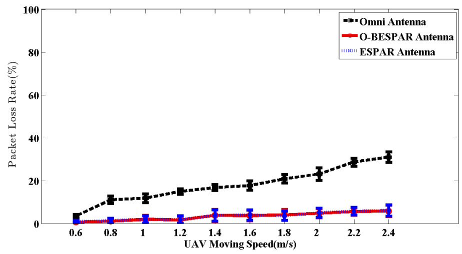

(c) Packet loss rate of link UAV-1 to base station

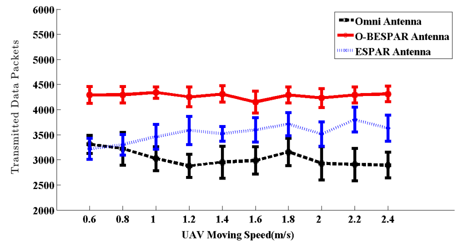

(d) Data packets transmitted by UAV-3

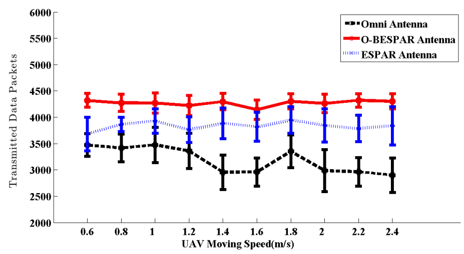

(e) Data packets transmitted by UAV-2

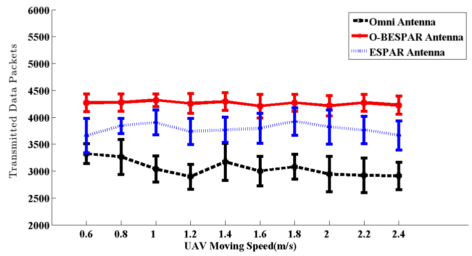

(f) Data packets transmitted by UAV-1

Figure 4.4: Packet loss rate and transmitted data packets with omni, ESPAR and O-BESPAR antenna in grid topology by random walk

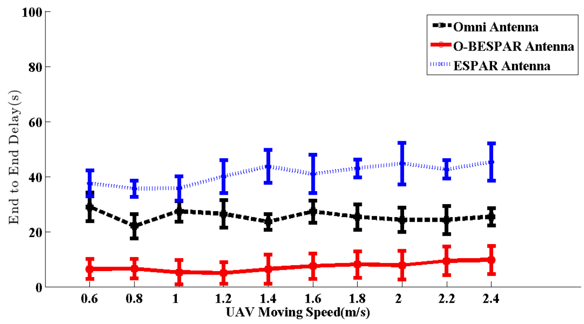

Figure 4.5: End to end delay in grid topology by random walk

For UP-DOWN movement scenario, the packet loss rate of two UAV links and the Air-Ground link with different antennas is presented by Figure 4.6(a), (b) and (c). The packet loss rate increases with increase in the UAV speed. For single ESPAR and O-BESPAR antenna, *HELLO* and *ACK* messages continue to steer the UAV's beamforming such that the main lobes are always pointed to each other. Both of them can mitigate the interference by beam steering and directivity, so both have much less packet loss rate (about 28% to 50%) than omni antenna. Figure 4.6(d), (e) and (f) illustrate the goodput analysis for UAV-3, UAV-2 and UAV-1. UAVs with O-BESPAR antenna transmit more data packets as compared with omni and single ESPAR antenna across the range of speed. At high speed, the data packets transmitted by O-BESPAR antenna is 20% higher than omni and single ESPAR antenna. While at low speed, O-BESPAR antenna shows gain of 33% and 18% in goodput as compared with omni and single ESPAR antenna. Note that the difference in goodput decreases with increase in the speed of the UAVs. This is because the UAVs move in a fixed path, higher speeds provides more chances of data transmission even for the omni antenna scenario.

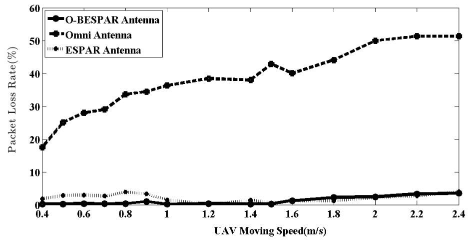

(a) Packet loss rate of Link UAV-3 to UAV-2

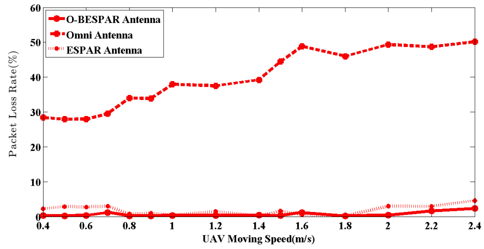

(b) Packet loss rate of link UAV-2 to UAV-1

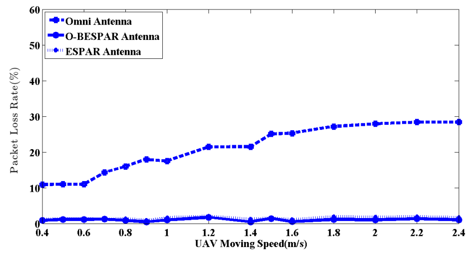

(c) Packet loss rate of link UAV-1 to base station

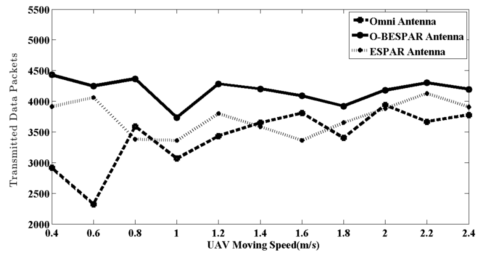

(d) Data packets transmitted by UAV-3

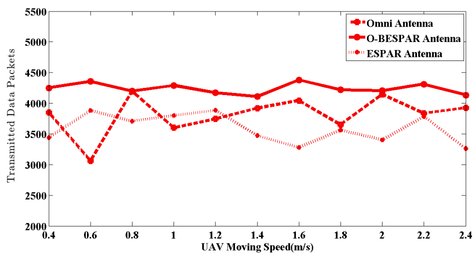

(e) Data packets transmitted by UAV-2

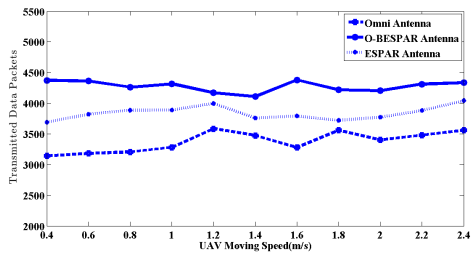

(f) Data packets transmitted by UAV-1

Figure 4.6: Packet loss rate and number of transmitted data packets with omnidirectional, single ESPAR and O-BESPAR antenna in UP-DOWN movement

The end to end delay of different types of antenna in UP-DOWN scenario are shown in Figure 4.7. The delay of all antennas decreases with increase of

UAV speeds because they have more frequenct contact with each other. As shown, O-BESPAR antenna has the smallest delay and single ESPAR antenna has the biggest since it has to rotate the unique beam to search the neighbor in 360 degrees.

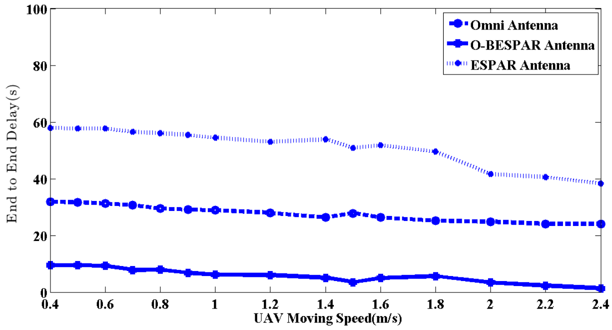

Figure 4.7: End to end delay in UP-DOWN movement

The packet loss rate of UAVs with omni, single ESPAR and O-BESPAR antenna is shown in Figure 4.8 for the square random walk scenario. The UAVs equipped with ESPAR and O-BESPAR antenna lost less than 7% of the data packets as compared to about 50% for the omni antenna. multiple factors contribute to this behavior. Firstly, the omni antennas equipped UAVs are subjected to more interference due to frequent roaming in the same broadcast domain. Secondly, the range of the omni antenna is limited (35m) as compared to the directional antenna. So there are less chances for neighbor discovery and data transfer as compared with the other antenna modules. The goodput of UAVs with three types of antenna is illustrated in Figure 4.9. O-BESPAR antenna demonstrates the highest goodput among the three antenna types. The end to end delay is presented by Figure 4.10. O-BESPAR antenna achieves 30 seconds less than the single ESPAR antenna which has the longest delay.

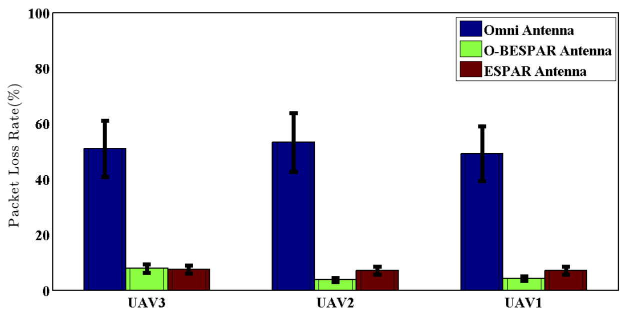

Figure 4.8: UAVs data packet loss rate in square random walk

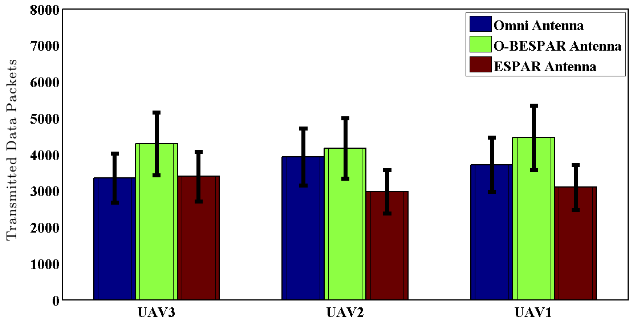

Figure 4.9: The Goodput analysis in square random walk

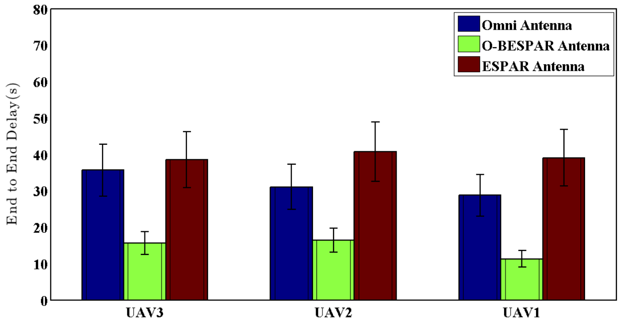

Figure 4.10: The end to end delay in square random walk

5 Conclusion

In this paper, we investigated the use of a hybrid antenna that combines isotropic omni and bi-directional antennas to improve the neighbor discovery mechanism and the transmission performance in AWSNs. We presented its design structure and a communication protocol, which separates the data and control transmissions over the omni and directional modules, respectively. O-BESPAR antenna is able to provide bi-directional communications through beamforming. The directivity of O-BESPAR antenna guarantees that the communications between two UAVs or UAV and base station have no interference to the others. We presented extensive simulations incorporating both realistic scenarios and 3D radio characterization and demonstrated the efficacy of our proposed antenna.

In our future work we plan to fabricate an O-BESPAR antenna based on the design presented in this paper. We also plan to conduct field experiments by mounting this antenna on a number of MikroKopter HexaKopters [1]. This will enable us to study the performance of the proposed antenna and protocol in a real-world setting.

Bibliography

[1] http://www.mikrokopter.de/, 04 2012.

[2] http://www.mikrokopter.de/ucwiki/en/flighttime, 04 2012.

[3] N. Ahmed, S.S. Kanhere, and S. Jha. Link characterization for aerial wireless sensor networks. In *GLOBECOM Workshops (GC Wkshps), 2011 IEEE*, pages 1274–1279. IEEE, 2011.

[4] S. Bandyopadhyay, K. Hasuike, S. Horisawa, and S. Tawara. An adaptive mac protocol for wireless ad hoc community network (wacnet) using electronically steerable passive array radiator antenna. In *Global Telecommunications Conference, 2001. GLOBECOM'01. IEEE*, volume 5, pages 2896–2900. IEEE, 2001.

[5] V. Barousis, A.G. Kanatas, A. Kalis, and C. Papadias. A stochastic beamforming algorithm for espar antennas. *Antennas and Wireless Propagation Letters, IEEE*, 7:745–748, 2008.

[6] A. Constantine. *Antenna theory: analysis and design.* Wiley, 2005.

[7] A. Cornejo, N. Lynch, S. Viqar, and J.L. Welch. Neighbor discovery in mobile ad hoc networks using an abstract mac layer. In *Communication, Control, and Computing, 2009. Allerton 2009. 47th Annual Allerton Conference on*, pages 1460–1467. IEEE, 2009.

[8] H.N. Dai. Throughput and delay in wireless sensor networks using directional antennas. In *Intelligent Sensors, Sensor Networks and Information Processing (ISSNIP), 2009 5th International Conference on*, pages 421–426. IEEE, 2009.

[9] K. Dantu, B. Kate, J. Waterman, P. Bailis, and M. Welsh. Programming micro-aerial vehicle swarms with karma. In *Proceedings of the 9th ACM Conference on Embedded Networked Sensor Systems*, pages 121–134. ACM, 2011.

[10] K. Dantu, M. Rahimi, H. Shah, S. Babel, A. Dhariwal, and G.S. Sukhatme. Robomote: enabling mobility in sensor networks. In *Proceedings of the 4th international symposium on Information processing in sensor networks*, page 55. IEEE Press, 2005.

[11] T. Furukawa, M. Bandai, H. Yomo, S. Obana, and T. Watanabe. Multilobe multicast using directional antenna for network coding in multi-rate ad hoc networks. In *Proceeding of the 14th IPSJ DICOMO Symposium*, pages 164–170, 2010.

[12] M.A. Goodrich, B.S. Morse, D. Gerhardt, J.L. Cooper, M. Quigley, J.A. Adams, and C. Humphrey. Supporting wilderness search and rescue using a camera-equipped mini uav. *Journal of Field Robotics*, 25(1-2):89–110, 2008.

[13] K. Gyoda and T. Ohira. Design of electronically steerable passive array radiator (espar) antennas. In *Antennas and Propagation Society International Symposium, 2000. IEEE*, volume 2, pages 922–925. IEEE, 2000.

[14] T. Hassan, A. Kausar, H. Umair, and M.A. Anis. Gain optimization of a seven element espar antenna using quasi-newton method. In *Microwave Technology & Computational Electromagnetics (ICMTCE), 2011 IEEE International Conference on*, pages 293–296. IEEE, 2011.

[15] S. Hauert, S. Leven, J.C. Zufferey, and D. Floreano. Communication-based swarming for flying robots. In *Proc. Intl. Conf. Robotics and Automation Workshop on Network Science and Systems*, 2010.

[16] H. Kawakami and T. Ohira. Electrically steerable passive array radiator (espar) antennas. *Antennas and Propagation Magazine, IEEE*, 47(2):43–50, 2005.

[17] P. Li, C. Zhang, and Y. Fang. The capacity of wireless ad hoc networks using directional antennas. *Mobile Computing, IEEE Transactions on*, 10(10):1374–1387, 2011.

[18] D. Lymberopoulos, Q. Lindsey, and A. Savvides. An empirical characterization of radio signal strength variability in 3-d ieee 802.15. 4 networks using monopole antennas. *Wireless Sensor Networks*, pages 326–341, 2006.

[19] A. Nasipuri, S. Ye, J. You, and RE Hiromoto. A mac protocol for mobile ad hoc networks using directional antennas. In *Wireless Communications and Networking Conference, 2000. WCNC. 2000 IEEE*, volume 3, pages 1214–1219. IEEE, 2000.

[20] V. Navda, A.P. Subramanian, K. Dhanasekaran, A. Timm-Giel, and S. Das. Mobisteer: using steerable beam directional antenna for vehicular network access. In *Proceedings of the 5th international conference on Mobile systems, applications and services*, pages 192–205. ACM, 2007.

[21] T. Ohira and K. Gyoda. Electronically steerable passive array radiator antennas for low-cost analog adaptive beamforming. In *Phased Array Systems and Technology, 2000. Proceedings. 2000 IEEE International Conference on*, pages 101–104. IEEE, 2000.

[22] R. Schlub, J. Lu, and T. Ohira. Seven-element ground skirt monopole espar antenna design from a genetic algorithm and the finite element method. *Antennas and Propagation, IEEE Transactions on*, 51(11):3033–3039, 2003.

[23] A. SINHA, A. TSOURDOS, and B. WHITE. Multi uav coordination for tracking the dispersion of a contaminant cloud in an urban region. *European journal of control*, 15(3-4):441–448, 2009.

[24] G. Sirigineedi, A. Tsourdos, B.A. White, and R. Zbikowski. Modelling and verification of multiple uav mission using smv. *Arxiv preprint arXiv:1003.0381*, 2010.

[25] J. Valente, D. Sanz, A. Barrientos, J. Cerro, Á. Ribeiro, and C. Rossi. An air-ground wireless sensor network for crop monitoring. *Sensors*, 11(6):6088–6108, 2011.

[26] I. Vasilescu, K. Kotay, D. Rus, L. Overs, P. Sikka, M. Dunbabin, P. Chen, and P. Corke. Krill: An exploration in underwater sensor networks. In *The Second IEEE Workshop on Embedded Networked Sensors, 2005. EmNetS-II*, pages 151–152. IEEE, 2005.

[27] F.N. Webber and R.E. Hiromoto. Assessing the communication issues involved in implemening high-level behaviors in unmanned aerial vehicles. In *Military Communications Conference, 2006. MILCOM 2006. IEEE*, pages 1–7. IEEE, 2006.